Macroscopic Dark Matter under siege: from White Dwarf Data to Gravitational Wave Detectors

Fa Peng Huang

Sun Yat-sen University, School of Physics and Astronomy,
TianQin center

New directions EXploring the Unknown beyond the Standard Model (NEXUS 2026)
@Tsung-Dao Lee Institute, 2026.09.14

Motivation: DM theory and experiments status

What is the microscopic nature of DM?

How DM is produced?

How to detect?

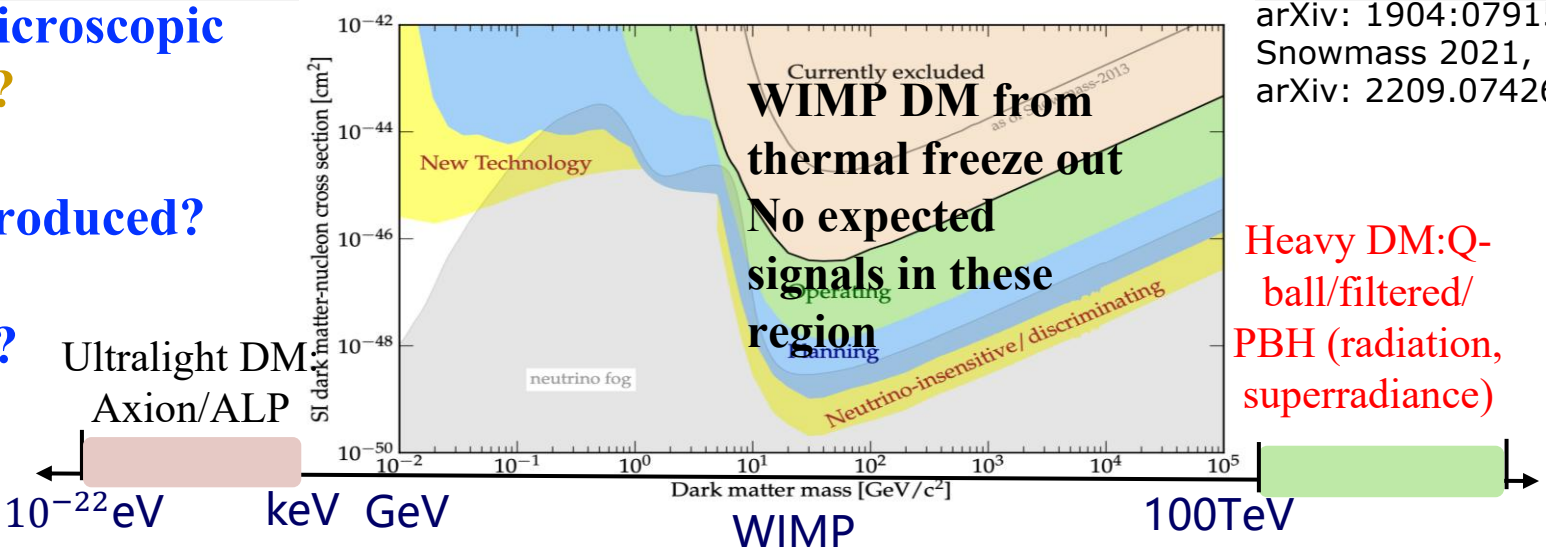

arXiv: 1904:07915
Snowmass 2021,
arXiv: 2209.07426

- **new DM production mechanism beyond thermal freeze out:**
  cosmic phase transition, PBH Hawking radiation, Kerr PBH superradiance…
- **new detection method: GW detector like PTA, LIGO, LISA/TianQin/Taiji**

DM may have Imprints at GW experiments

GW experiments

LISA/TianQin/Taiji ~2034

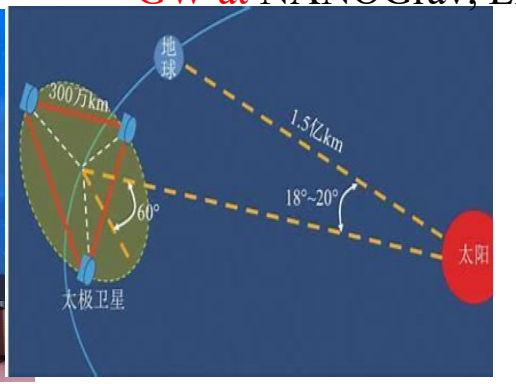

"TianQin"
"Harpe in space"

2023 June 29th: possible hints of stochastic GW at NANOGrav, EPTA, InPTA, Parkes PTA, CPTA

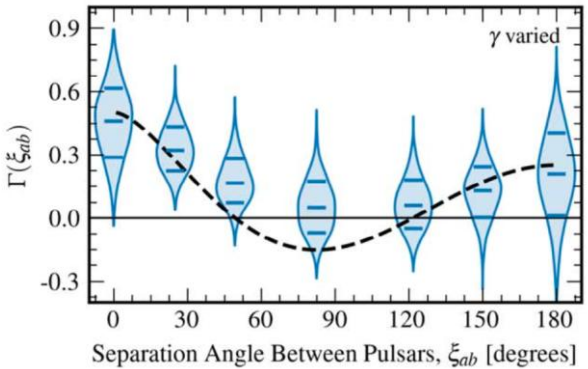

[Fundamental physics and cosmology with TianQin](#)
Living Rev.Rel. 29 (2026) 1, 1,arXiv: 2502.20138

FAST

SKA

Motivation: DM Imprints at GW experiments

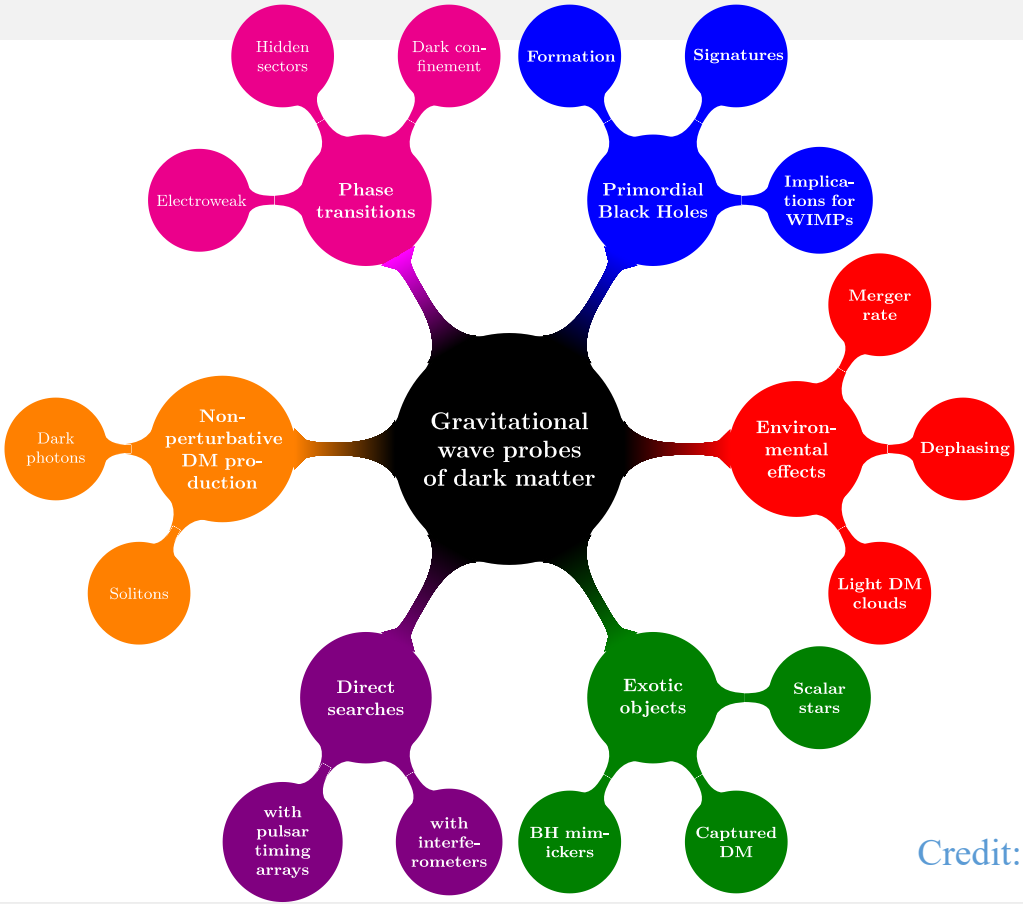

Credit: Gianfranco Bertone et. al.

Ultralight DM

GW signal of ultralight DM from black hole: gravitational atom from superradiance

1. Axions can annihilate to GW
2. Energy-level transition of gravitational atom can radiate GW

Jing Yang, FPH Phys.Rev.D 108 (2023) 10, 103002
Jing Yang, Ning Xie, FPH JCAP 11 (2024) 045
Ning Xie, FPH Sci. China-Phys. Mech. Astron. 67, 210411
Ning Xie, FPH Phys.Rev.D 112 (2025) 5, 055028
Zhong-hao Luo, FPH, Pengming Zhang, Chen Zhang, arXiv: 2601.10552,SCMPA 2026

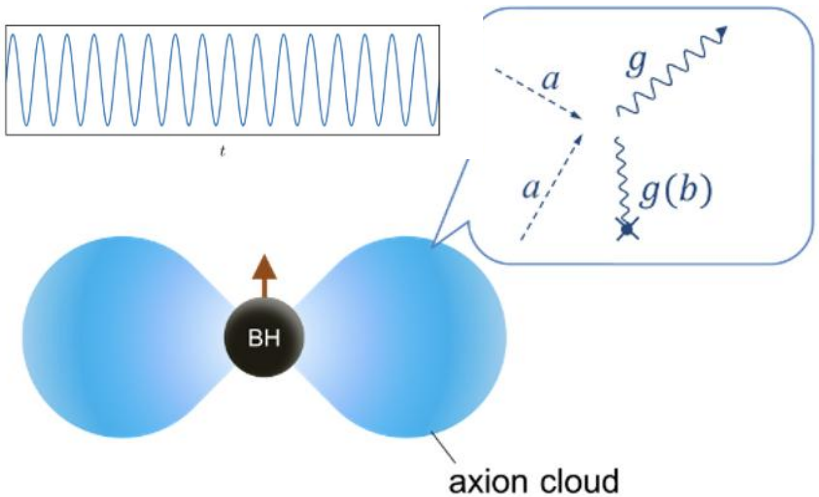

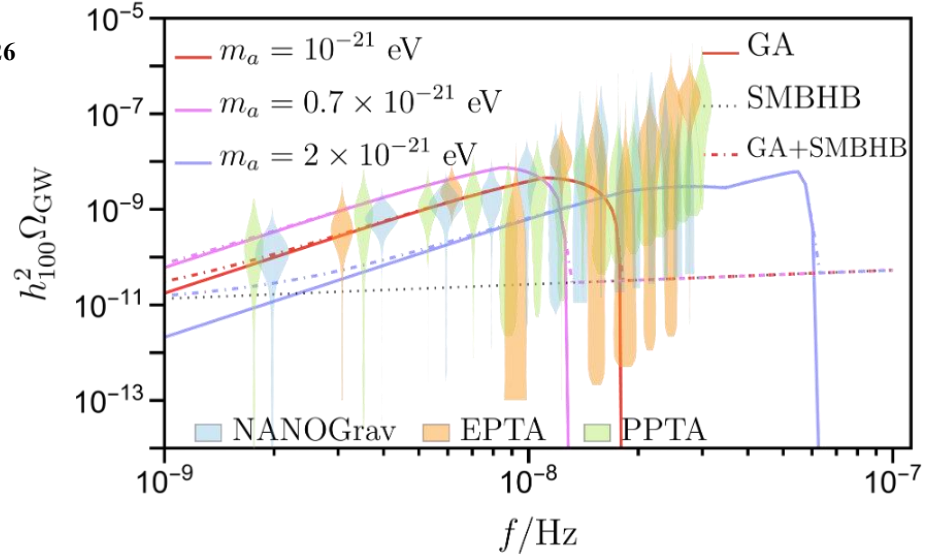

Heavy DM: new production mechanism

1. Renaissance of quark nugget DM idea by E. Witten: Bubble wall in FOPT can be the "filter" to obtain the needed heavy DM avoiding the unitarity constraints with phase transition GW signals.

J. Baker, J. Kopp, Andrew J. Long,
Phys.Rev.Lett. 125 (2020) 15, 151102

FOPT in the early universe	Coffee making process
Bubble wall	Filter
Case I:(gauged) Q-ball DM	Large coffee beans
Case II: filtered DM	Coffee
Case III: PBH	Remants
Phase transition GW	**Aroma**

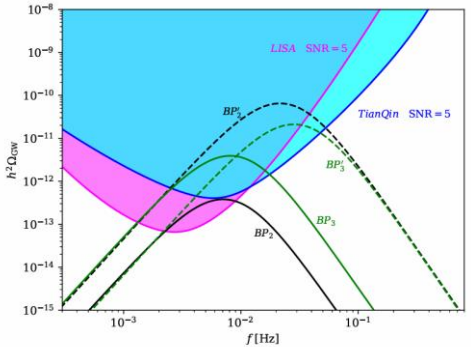

FPH, Chong Sheng Li, Phys.Rev. D96 (2017) no.9, 095028
Siyu Jiang, FPH, Chong Sheng Li, Phys.Rev.D 108 (2023) 6, 063508
Siyu Jiang, FPH, Pyungwon Ko, JHEP 07 (2024) 053
FPH, Chikako, Aidi, Phys.Rev.D 113 (2026) 5, 055013
Siyu Jiang, FPH, JCAP 06 (2025) 023
Dayun Qiu, Siyu Jiang, FPH, JHEP 02 (2026) 112

2. Heavy DM from PBH Hawking radiation, Kerr PBH superradiance

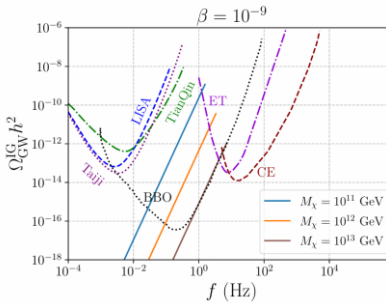

Beyond phase transition GW signals

Low Flux problem for heavy DM direct detection

For fixed local DM density, the number density and encounter rate fall inversely with the object mass.

$$n_{DM} = \rho_{DM} / M_{DM}$$

As DM mass increases

- particle-like searches lose flux rapidly
- macroscopic probes need larger effective exposure
- traditional WIMP searches motivate complementary probes

Low flux is one central challenge; the rest of the talk is a strategy for defeating it.

Beyond phase transition GW signals

Heavy or macroscopic DM is difficult since its flux falls as 1/M.
The solution is to make the detector astrophysically large or precise.

COMPACT STARS

Huge target × long exposure time

White Dwarf/Neutron star

Heavy DM can deposit enough energy to ignite a white dwarf (WD) or trigger a neutron-star (NS) superburst.

SPACE INTERFEROMETERS

Astronomical baseline × laser precision

GW detector in space: TianQin/Taiji/LISA

A macroscopic DM flyby produces differential acceleration of the test masses (TMs)—an impulse-like Doppler/TDI signal.

Compact stars provide exposure; space interferometers provide precision and astronomical baseline.
Together they put macroscopic DM "under siege."

Unified multi-messenger search strategy

ROADMAP

The same macroscopic object can be constrained by stellar ignition and detected through precision interferometry.

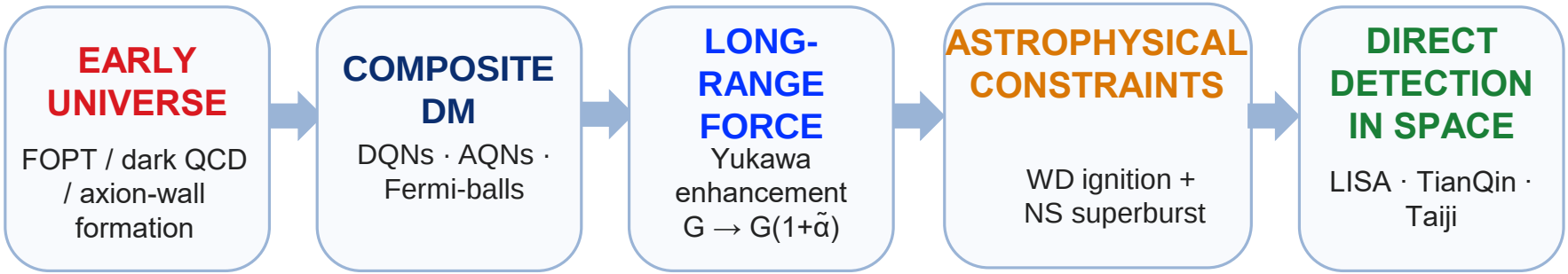

DM production mechanism
Phase transition GW (stochastic)

DM mass, interaction
impulse-like TDI signal.

We go from formation physics in the early Universe to astrophysical constraints to direct detection and parameter reconstruction.

DM Direct detection on GW experiments

Probing heavy DM frontier presents a distinct experimental challenge: as the mass increases, number density drops precipitously, rendering direct detection experiments on earth effectively blind to the resulting low flux.

To overcome this "flux barrier", one can utilize astrophysical scales. Compact objects like WDs, acting as vast, long-exposure detectors, offer a powerful alternative.

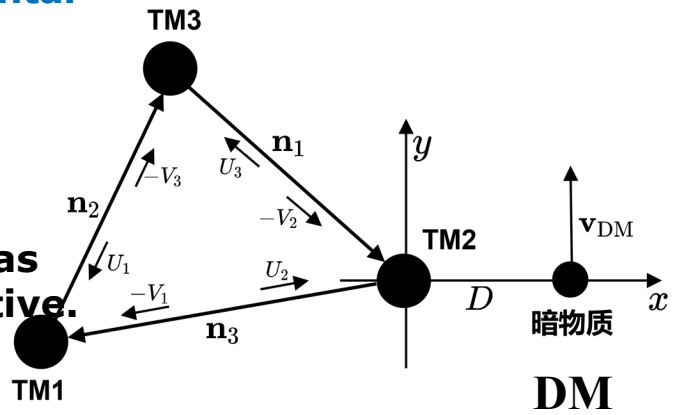

GW detector in space is a natural big (astrophysical scale) and precise (high precision laser interferometer) DM detector.

We apply this detection scheme to macroscopic DM.

As a heavy DM object passes near the detector, its new interaction with TM causes differential acceleration among the test masses of GW detectors, producing a detectable Doppler signal.

Multimessenger search strategy for composite dark matter with white dwarf data and gravitational wave detectors, Aidi Yang, and FPH, arXiv:2511.23263, Phys. Rev. D 114, 053008 (2026), and work in progress

Composite DM with long-range interaction

For various macroscopic or composite DM models, the DM is composite of dark fermions X.
We show three representative models formed by FOPT below for a broad class of composite DM models, where the DM mass can be parameterized as

$$M_{\rm DM} = \varepsilon \times \frac{4\pi}{3} R_{\rm DM}^3$$

(a) Dark quark nuggets (DQNs): Phys. Rev. D **99**, 055047 (2019)
(b) Axion quark nuggets (AQNs): JCAP **10**, 010 (2003)
(c) Fermi-balls: Phys. Rev. D **102**, 075028 (2020),

$$\mu_{\rm eq} = \left(\frac{6\pi^2\varepsilon}{g_{\rm dof}}\right)^{1/4}, \quad N_{\rm DM} = \frac{2g_{\rm dof}}{9\pi}\mu_{\rm eq}^3 R_{\rm DM}^3$$

We introduce a long-range scalar mediator that couples the DM via $y_{\rm DM}\bar{X}\phi X$ and the nucleons via $y_{\rm SM}\bar{n}\phi n$, such that an additional Yukawa attractive potential arises between two objects $i, j \in \{\rm SM, DM\}$,

$$V_{i-j} = -M_i M_j \frac{G}{r}\left(1 + \delta_i\delta_j e^{-m_{\rm med}r}\right) \qquad \delta_i = \frac{y_i N_i}{\sqrt{4\pi G} M_i}$$

Composite DM with long-range interaction

We will assume the force range λ is larger than the typical lengths in this work, i.e., the radius of white dwarfs (WD) or neutron stars (NS), and the arm length of the GW detector; for instance, we take λ = 0.1 pc.

> Then the attractive potential between the DM and the nucleons is simply obtained by replacing the Newton constant in the gravitational potential by $G \to G(1+\tilde{\alpha})$ with
>
> $$\tilde{\alpha} = \delta_{\rm SM}\delta_{\rm DM}.$$

MICROSCOPE experiments: $|\delta_{\rm SM}| < 3 \times 10^{-6}$

Bullet cluster constraints: $\delta_{\rm DM}^2 < 2 \times 10^6 \left(\frac{M_{\rm DM}}{M_\odot}\right)^{-1/2} \left(\frac{v_{\rm DM}}{10^{-2}}\right)^2 e^{4\times10^{-3}\sqrt{\frac{M_{\rm DM}}{M_\odot}}\frac{\rm pc}{\lambda}}$

Two complementary responses to flyby DM

A compact star acts as a calorimeter; a space interferometer acts as a precision accelerometer.

1 · ENERGY DEPOSITION

DM transit → scattering → local heating → runaway fusion

Observable: survival / SN Ia / superburst rate

2 · DIFFERENTIAL ACCELERATION

Nearby flyby → test mass velocity perturbation → TDI signal

Observable: transient PSD / SNR / reconstructed parameters

The same DM creates both astrophysical constraints and laboratory-style direct-detection observables.

Runaway fusion of compact objects

Firstly, we briefly discuss the condition of triggering runaway fusion in a WD core and NS ocean. When DM passes a WD or NS, it may deposit energy through scattering with C or O ions. If the energy deposition $E_{\rm dep}$ is enough for the ions to overcome their mutual Coulomb barrier, the runaway fusion occurs.

- ✓ The first condition for fusion is that the energy deposition must raise the temperature of a certain area above some critical value $T_{\rm crit} \sim$ MeV.
- ✓ The second condition is that the timescale for cooling due to thermal diffusion has to be longer than the timescale corresponding to the heating due to fusion.

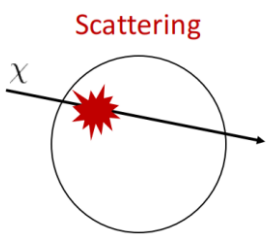

The former increases with the size of the heated region but the latter is independent of the size of the region; therefore, there is a critical size λ_T beyond which the heat cannot be efficiently diffused.
The ignition condition reads

$$E_{\rm dep} \geq E_{\rm trig} \equiv \frac{4\pi}{3}\rho\lambda_T^3\left(\rho, T_{\rm crit}\right)\bar{c}_p\left(\rho, T_{\rm crit}\right)T_{\rm crit}$$

Runaway fusion of compact objects

$$E_{\rm dep} \geq E_{\rm trig} \equiv \frac{4\pi}{3}\rho\lambda_T^3\left(\rho, T_{\rm crit}\right)\bar{c}_p\left(\rho, T_{\rm crit}\right)T_{\rm crit}$$

It is often assumed that DM triggers the ignition near the center of a C/O WD. Obtaining the density profile of WDs requires solving the Tolman–Oppenheimer–Volkoff (TOV) equation. We use the analytic fit of the WD-mass central density relationship

$$1+\left(\frac{\rho_{\rm WD}}{1.95\times10^6\ {\rm g/cm^3}}\right)^{\frac{2}{3}} \approx \left[\sum_{i=0}^{6} c_i \left(\frac{M_{\rm WD}}{M_\odot}\right)^i\right]^{-2}$$

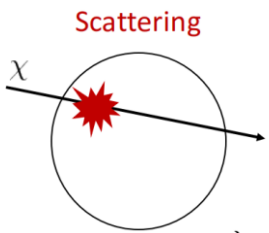

The trigger length λ_T is obtained by comparing the nuclear energy generation rate and the heat diffusion rate. However, the specific nuclear energy generation rates of the WD generally require numerical simulation, and we use an analytical scaling relation

$$\lambda_T = \begin{cases} \lambda_1\left(\frac{\rho}{\rho_1}\right)^{-2}, & \rho \leq \rho_1\ , \\ \lambda_1\left(\frac{\rho}{\rho_1}\right)^{\ln(\lambda_2/\lambda_1)/\ln(\rho_2/\rho_1)}, & \rho_1 < \rho \leq \rho_2 \end{cases}$$

We take 4361 WDs in Montreal White Dwarf Database with known lifetimes and masses spanning $0.8 < M_{\rm WD}/M_\odot < 1.4$.

The update with 4361 WDs

Density structure, trigger length and the non-degenerate envelope determine whether a DM transit can ignite the star.

4,361
WHITE DWARFS
Montreal White Dwarf Database

0.8–1.4 $M_\odot$
MASS RANGE
objects with known mass and lifetime

$\rho_{env} = 10^{-3}\rho_{WD}$
DENSITY THRESHOLD
conservative non-degenerate envelope

M_{WD} mass → ρ_c central density → λ_T trigger size → E_{trig} ignition energy

The updated treatment is both more data-driven and more conservative than earlier simplified estimates.

Runaway fusion of compact objects

Unlike WD, the thermal nuclear runaway causes the NS to undergo a superburst instead of a supernova. The outer layer of NS consists of an ocean of heavy elements, where the mass fraction of carbon is approximately 10% . For NSs, the precise nature of the initiation of a superburst is still unclear. However, similar to the WDs, the trigger length is also derived by comparing the carbon fusion rate with the heat diffusion rate.

The superbursts source 4U 1820-30 is used to place constraints on the composite DM.

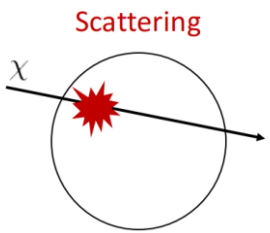

NEUTRON-STAR SUPERBURSTS

In a neutron star, runaway carbon burning produces a superburst rather than a supernova.

4U 1820−30 **Representative superburst source**

- Carbon mass fraction in the ocean ≈ 10%
- Maximum ignition column depth ≈ 4×10^{13} g cm^{-2}
- Recurrence time t_{rec} = 2.5 yr
- Galactic position ≈ 1.2 kpc

Higher density → stronger focusing and typically stronger constraints

NS observations provide a complementary astrophysical handle on the same underlying macroscopic DM population.

WDs and NSs probe different density and ignition conditions, making the astrophysical exclusions more robust.

ASTROPHYSICAL RATE

Ignition is not enough: the event rate closes the loop

A viable constraint requires both successful ignition and at least one expected transit through the observed compact-object population.

Long-range attraction increases focusing

The maximum impact parameter $b_{\max}$ grows with $\tilde{\alpha}$, bringing more macroscopic objects through the star.

$$N_{enc} = \Sigma_i \, \Gamma_{enc} \, \tau_i$$

6.25×10^{18} g

Max WD-CONSTRAINED MASS for $\tilde{\alpha} = 0$

6.46×10^{20} g

WITH LONG-RANGE FOCUSING for $\tilde{\alpha} = 100$

Focusing and event rates extend the astrophysical sensitivity by about two orders of magnitude in mass.

Updated WD data

A refined non-degenerate-envelope treatment and the expanded WD sample produce a conservative revised bound.

$$\sigma_{DM-A}/\,M_{DM} \gtrsim 7.3 \times 10^{-11}\ \mathrm{cm}^2\,\mathrm{g}^{-1}$$

MAIN ASTROPHYSICAL RESULT

~100× larger
than Graham et al. benchmark

~10^6× larger
than Singh Sidhu et al. benchmark

~300× smaller
than Raj et al. benchmark

The astrophysical benchmark is updated in a conservative direction before comparing with interferometer reach.

Constraints from supernova and superburst

Constraints from astrophysical detections:

DM may interact with nucleons on the surface of white dwarfs or neutron stars, thereby triggering supernovae or superbursts.

In addition to the ignition, it is important to investigate the event rate at WDs/NSs. The encounter rate between DM and WD/NS relies on the maximum impact factor b_{max}

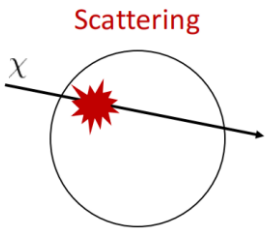

$$\Gamma_{\rm enc}^{\rm DM}(r) = f_{\rm DM}\frac{\rho_{\rm DM}(r)}{M_{\rm DM}} v_{\rm DM}(r)\pi b_{\rm max}^2$$

The expected number of DM passing through the WDs is

$$N_{\rm enc}^{\rm WD} = \sum_i \Gamma_{\rm enc}^{\rm DM}\tau_{{\rm WD},i}$$

For NSs, the τ_{WD} has to be replaced by t_{rec}.

As more DM is focused, constraints are amplified when introducing the Yukawa interaction. The maximum value of DM mass to be constrained by WDs is 6.25×10^{18} g and 6.46×10^{20} g for $\tilde{\alpha} = 0$ and $\tilde{\alpha} = 100$, respectively.

DM Direct detection by GW experiments

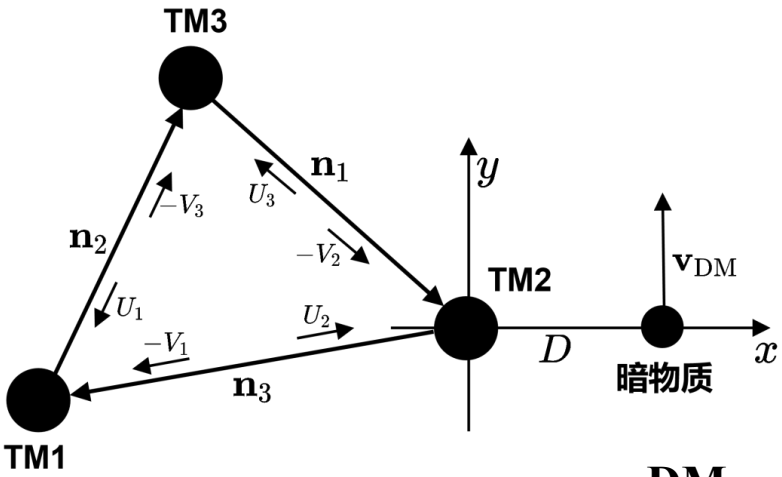

In the scenario where DM transits near a GW detection satellite, we assume the process occurs within the x − y plane, with the DM moving along the y-direction. The long-range Yukawa interaction results differential acceleration of TM

$$\mathbf{g}(t) = \frac{\tilde{G}M_{\rm DM}}{D^2}\frac{1}{\left[1+\left(\frac{v_{\rm DM}t}{D}\right)^2\right]^{3/2}}\begin{pmatrix}1\\ \frac{v_{\rm DM}t}{D}\\ 0\end{pmatrix}$$

$$\longrightarrow \quad \mathbf{v}(t,D) = \frac{\tilde{G}M_{\rm DM}}{Dv_{\rm DM}}\begin{pmatrix}1+\frac{v_{\rm DM}t/D}{\sqrt{1+v_{\rm DM}^2t^2/D^2}}\\ -\frac{1}{\sqrt{1+v_{\rm DM}^2t^2/D^2}}\\ 0\end{pmatrix}$$

$$r >> m_\phi^{-1}:$$

$$\tilde{G} = G(1+\tilde{\alpha}), \quad \tilde{\alpha} = \delta_{\rm SM}\delta_{\rm DM}.$$

$$\longrightarrow \quad U_1(t) = \mathbf{n}_2 \cdot \frac{\mathbf{v}_1(t) - \mathbf{v}_3(t - L/c)}{c}$$

$$V_1(t) = \mathbf{n}_3 \cdot \frac{\mathbf{v}_1(t) - \mathbf{v}_2(t - L/c)}{c}$$

permutation symmetry $1 \to 2 \to 3 \to 1$

DM Direct detection by GW experiments

In order to effectively cancel the laser noise, we employ the time-delay interferometry:

$$X(t) = U_1(t) + V_1(t) - U_1\left(t - \frac{2L}{c}\right) - V_1\left(t - \frac{2L}{c}\right) + U_2\left(t - \frac{3L}{c}\right) + V_3\left(t - \frac{3L}{c}\right) - U_2\left(t - \frac{L}{c}\right) - V_3\left(t - \frac{L}{c}\right)$$

$\omega = 2\pi f$

$$\tilde{X}(\omega) = \sqrt{\frac{2}{\pi}}\left(1 - \mathrm{e}^{4i\omega L/c}\right)\frac{\tilde{G}M_X}{cv_{\rm DM}^2}\sin\vartheta \times \left[K_0\left(\frac{D\omega}{v_{\rm DM}}\right)\sin\varphi - iK_1\left(\frac{D\omega}{v_{\rm DM}}\right)\cos\varphi\right] + \sqrt{\frac{8}{\pi}}\left(\mathrm{e}^{3i\omega L/c} - \mathrm{e}^{i\omega L/c}\right)\frac{\tilde{G}M_X}{cv_{\rm DM}^2}\sin\vartheta \times \left[K_0\left(\frac{D'\omega}{v_{\rm DM}}\right)\sin\varphi - iK_1\left(\frac{D'\omega}{v_{\rm DM}}\right)\cos\varphi\right] .$$

The power spectral density (PSD) of the DM signal

$$P(\omega) = \left\langle\left|\tilde{X}(\omega)\right|^2\right\rangle = \frac{1}{4\pi}\int \mathrm{d}\vartheta\sin\vartheta\int \mathrm{d}\varphi|\tilde{X}(\omega)|^2$$
$$= \frac{32}{3\pi}\left(\frac{\tilde{G}M_X}{cv_{\rm DM}^2}\right)^2\sin^2(\omega L/c) \times \left\{\left[K_0\left(\frac{D\omega}{v_{\rm DM}}\right)\cos(\omega L/c) - K_0\left(\frac{D'\omega}{v_{\rm DM}}\right)\right]^2 + \left[K_1\left(\frac{D\omega}{v_{\rm DM}}\right)\cos(\omega L/c) - K_1\left(\frac{D'\omega}{v_{\rm DM}}\right)\right]^2\right\} .$$

Direct detection by GW experiments

Parameter	LISA	TianQin	Taiji
Arm length L (10^9 m)	2.5	0.17	3
$P_{\rm oms}$ (10^{-12} m)	15	1	8
$P_{\rm acc}$ (10^{-15} m $\cdot$ s^{-2})	3	1	3
$T_{\rm obs}$ (yr)	4.5	2.5	5
Frequency range (Hz)	$[10^{-4}, 1]$	$[10^{-4}, 1]$	$[10^{-4}, 1]$

GW detector in space is a natural big (astrophysical scale) and precise (high precision laser interferometer) DM detector.

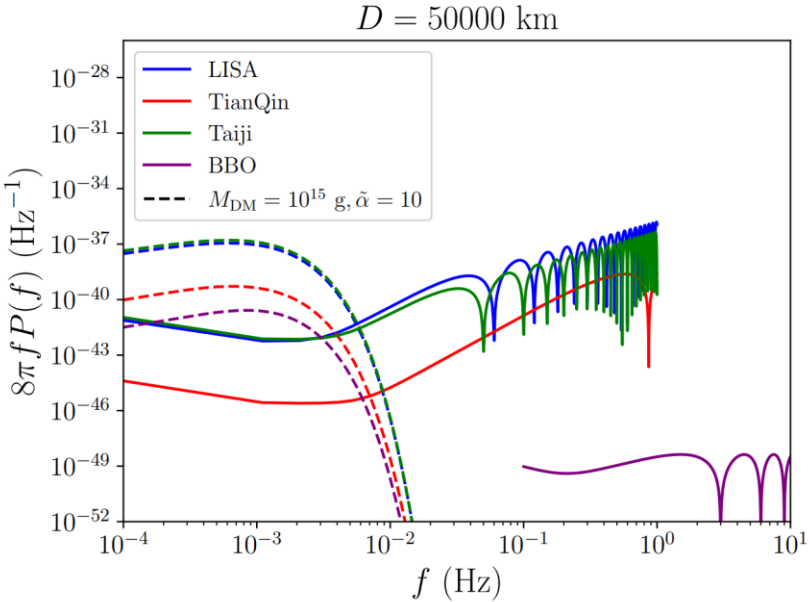

noise PSD in X channel:

$$S_X(f) = 16 \sin^2\left(\frac{2\pi f L}{c}\right)\left\{\left[3+\cos\left(\frac{4\pi f L}{c}\right)\right] S_{\rm acc}(f) + S_{\rm oms}(f)\right\}$$

$$S_{\rm oms}(f) = \left(\frac{2\pi f P_{\rm oms}}{c}\right)^2\left[1+\left(\frac{2\times 10^{-3}\ \text{Hz}}{f}\right)^4\right]\text{Hz}^{-1}$$

$$S_{\rm acc}(f) = \left(\frac{P_{\rm acc}}{2\pi f c}\right)^2\left[1+\left(\frac{0.4\times 10^{-3}\ \text{Hz}}{f}\right)^2\right]\times\left[1+\left(\frac{f}{8\times 10^{-3}\ \text{Hz}}\right)^4\right]\text{Hz}^{-1}$$

The signal PSD (dashed lines) of composite DM on the GW detectors in the X channel and the corresponding noise PSD (solid lines).

Direct detection by GW experiments

The expected number of DM passing through the detector:

$$N_{\rm enc}^{\rm GW} = \left(f_X \pi D^2 \rho_{\rm DM} v_{\rm DM} / M_X\right) T_{\rm obs}^i$$

We restrict at least one DM induced event will be expected during the lifetime of the experiments.

Signal-to-noise ratio

$$\mathrm{SNR} = \left(4 \int_0^\infty \mathrm{d}\omega \frac{P(\omega)}{S_n(\omega)}\right)^{\frac{1}{2}} \geq 10$$

We find that space-based GW experiments can cover most of the parameter ranges beyond these astrophysical limits. And its results depend only on the mass of DM and its interaction strength with ordinary matter.

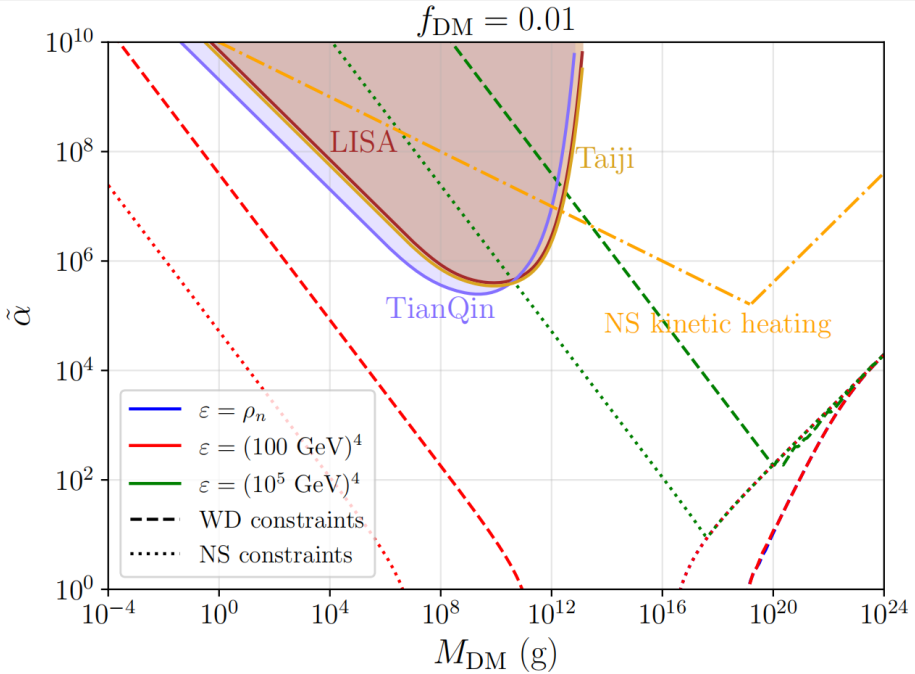

Sensitivity of GW detectors to composite DM with updated astrophysical constraints.

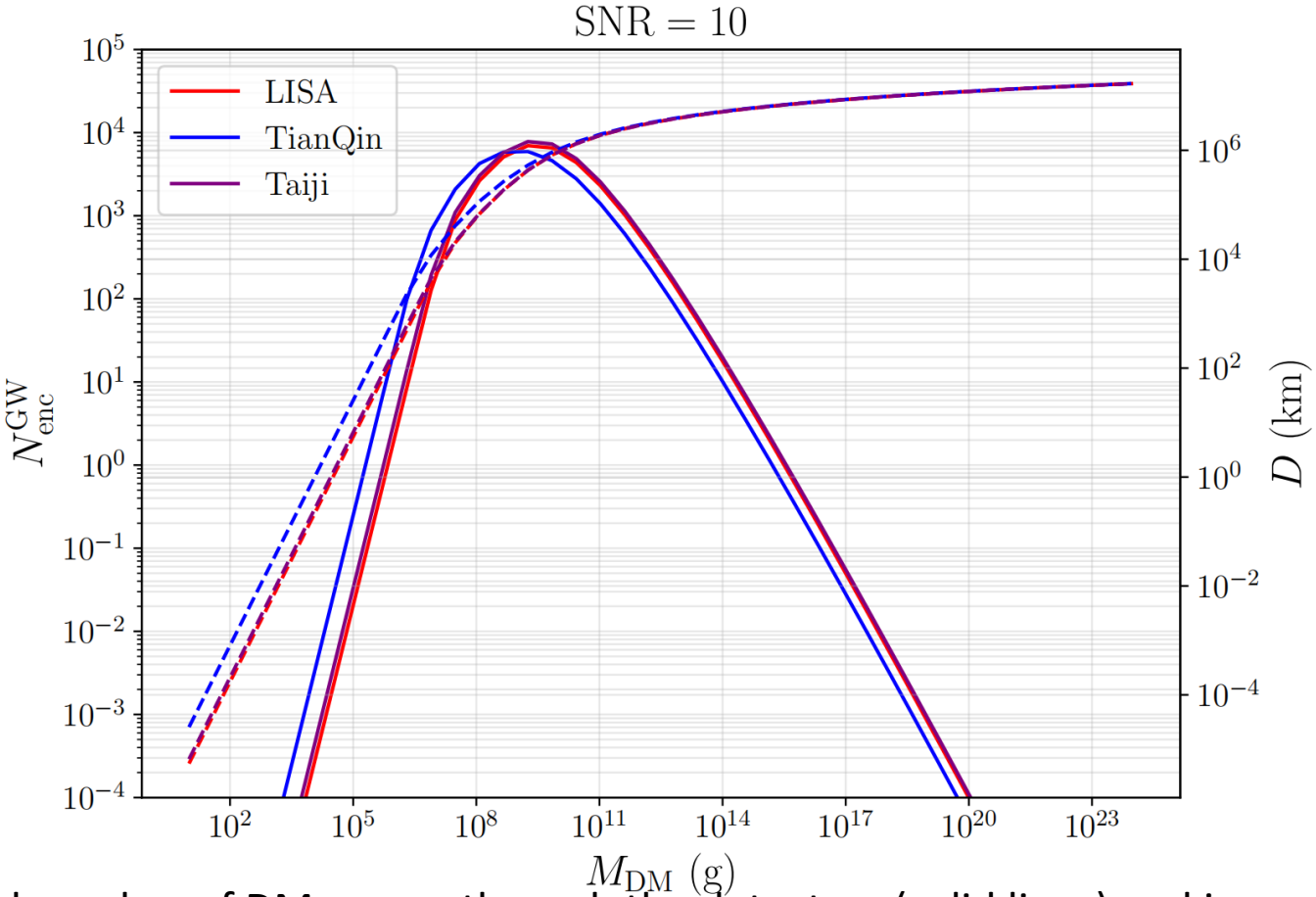

Expected number of DM passes through the detectors (solid lines) and impact factor (dashed lines) of composite DM as functions of DM mass in the X channel.

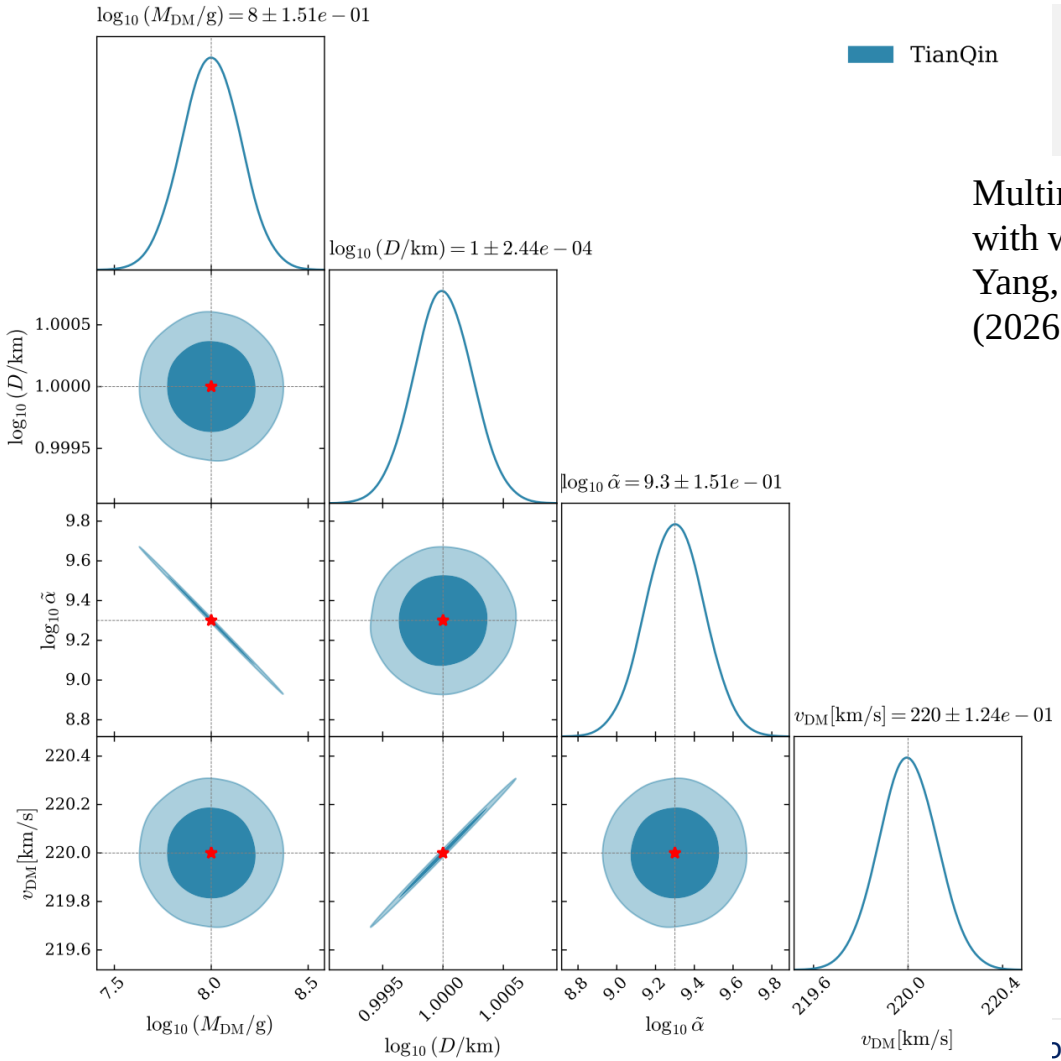

Multimessenger search strategy for composite dark matter with white dwarf data and gravitational wave detectors, Aidi Yang, and FPH, arXiv:2511.23263, Phys. Rev. D 114, 053008 (2026), and work in progress

Triangle plot of the Fisher analysis for a signal at TianQin induced by DM.

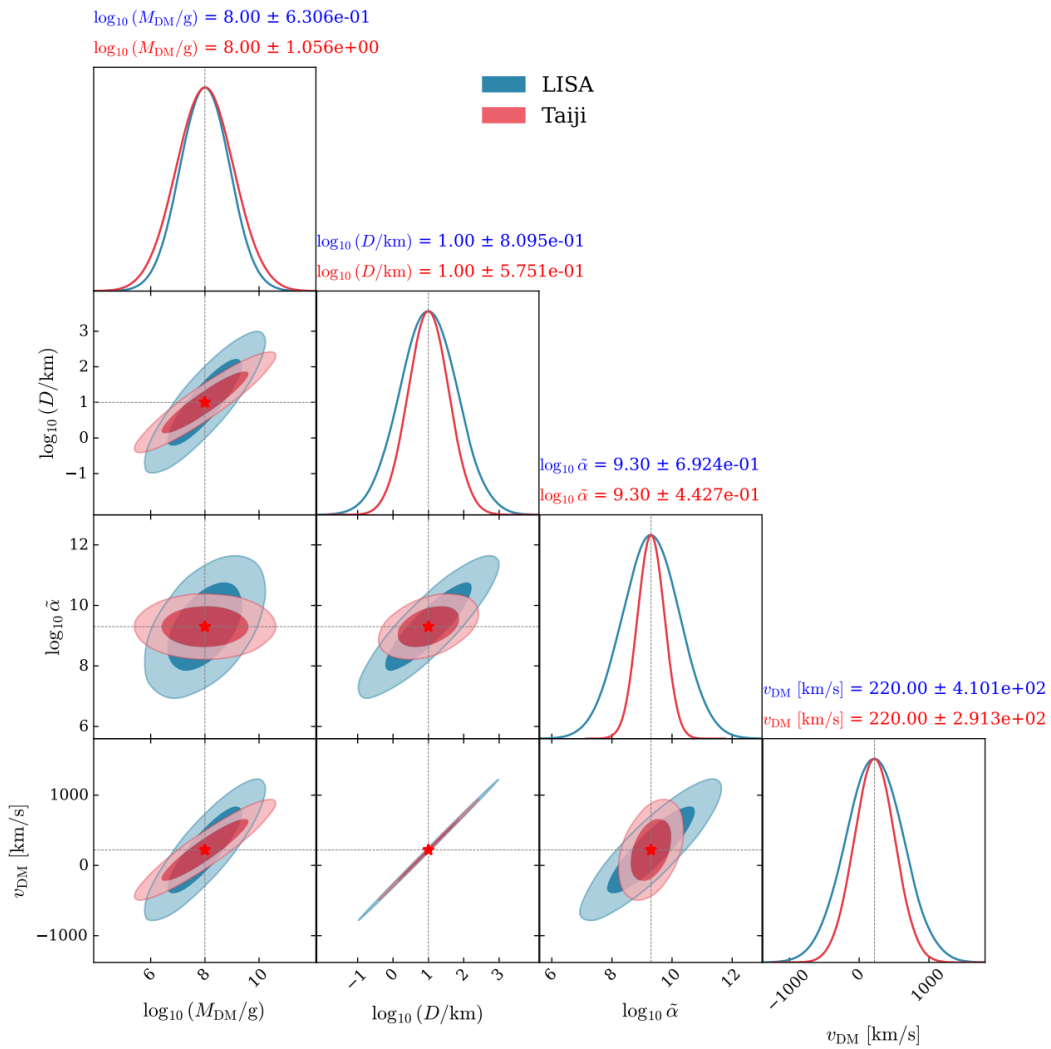
$\log_{10}(M_{\rm DM}/{\rm g})$ = 8.00 ± 6.306e-01
$\log_{10}(M_{\rm DM}/{\rm g})$ = 8.00 ± 1.056e+00
LISA
Taiji
$\log_{10}(D/{\rm km})$ = 1.00 ± 8.095e-01
$\log_{10}(D/{\rm km})$ = 1.00 ± 5.751e-01
$\log_{10}\tilde{\alpha}$ = 9.30 ± 6.924e-01
$\log_{10}\tilde{\alpha}$ = 9.30 ± 4.427e-01
$v_{\rm DM}$ [km/s] = 220.00 ± 4.101e+02
$v_{\rm DM}$ [km/s] = 220.00 ± 2.913e+02
$\log_{10}(M_{\rm DM}/{\rm g})$
$\log_{10}(D/{\rm km})$
$\log_{10}\tilde{\alpha}$
$v_{\rm DM}$ [km/s]

Summary:Unified multi-messenger search strategy

ROADMAP

The same macroscopic object can be constrained by stellar ignition and detected through precision interferometry.

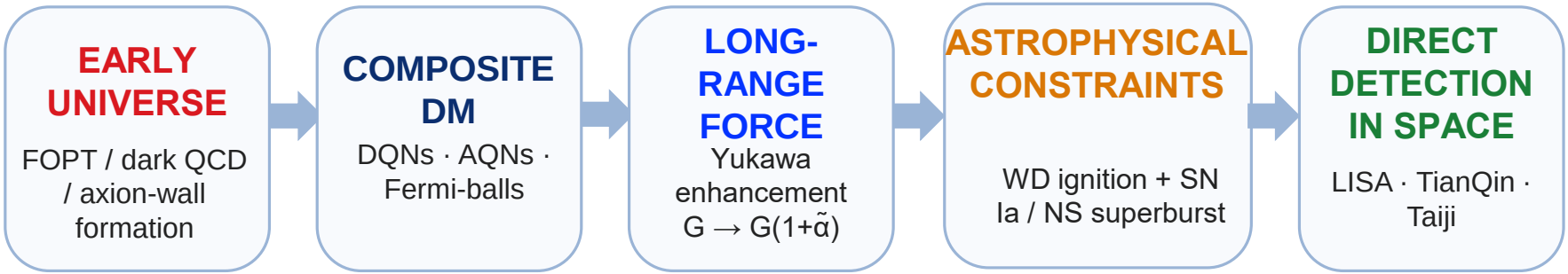

DM production mechanism
Phase transition GW (stochastic)

DM mass, interaction
impulse-like TDI signal.

We go from formation physics to astrophysical constraints to direct detection and parameter reconstruction.

Summary

GW detectors will help to explore DM production mechanism in the early universe, the distribution and propagation of DM in the late universe, and the microscopic nature of DM, such as its mass and interaction.

GW detector in space is a natural big (astrophysical scale) and precise (high precision laser interferometer) DM detector.

Thanks!
Comments are welcome.

Taking home message
Astrophysical scale + interferometric precision
= a new macroscopic/heavy DM detection

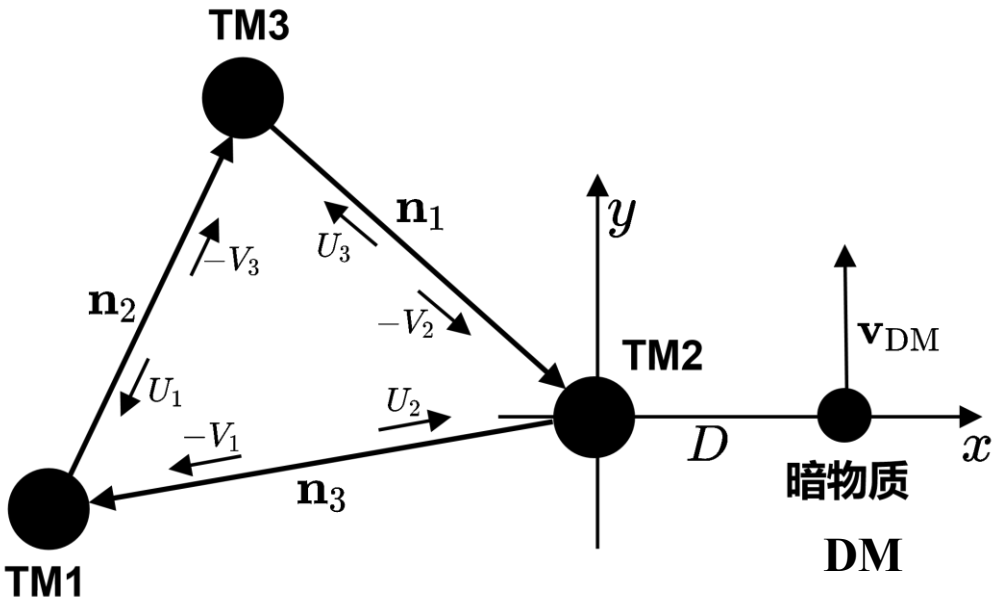

Direct detection on GW experiments

$$\alpha(t) = U_1(t) + V_1(t) + U_3(t - \frac{L}{c}) + V_2(t - \frac{L}{c}) + U_2(t - \frac{2L}{c}) + V_3(t - \frac{L}{c})$$
$$= -\mathbf{n}_1 \cdot \frac{\mathbf{v}(t, D) - \mathbf{v}(t - 3L/c, D)}{c} - 3\mathbf{n}_1 \cdot \frac{\mathbf{v}(t - 2L/c, D') - \mathbf{v}(t - L/c, D')}{c}$$

$$P_\alpha(\omega) = \left\langle |\tilde{\alpha}(\omega)|^2 \right\rangle = \frac{8}{3\pi} \left(\frac{\tilde{G} M_X}{c v_{\rm DM}^2} \right)^2 \sin^2 \left(\frac{\omega L}{2c} \right) \times \left\{ \left[K_0 \left(\frac{D\omega}{v_{\rm DM}} \right) \left(1 + 2\cos \left(\frac{\omega L}{c} \right) \right) - 3K_0 \left(\frac{D'\omega}{v_{\rm DM}} \right) \right]^2 + \left[K_1 \left(\frac{D\omega}{v_{\rm DM}} \right) \left(1 + 2\cos \left(\frac{\omega L}{c} \right) \right) - 3K_1 \left(\frac{D'\omega}{v_{\rm DM}} \right) \right]^2 \right\} ,$$

$$\zeta(t) = U_1(t - \frac{L}{c}) + V_1(t - \frac{L}{c}) + U_2(t - \frac{L}{c}) + V_2(t - \frac{L}{c}) + U_3(t - \frac{L}{c}) + V_3(t - \frac{L}{c})$$
$$= -\mathbf{n}_1 \cdot \left[\frac{\mathbf{v}(t - L/c, D) - \mathbf{v}(t - 2L/c, D)}{c} + \frac{\mathbf{v}(t - 2L/c, D') - \mathbf{v}(t - L/c, D')}{c} \right]$$

$$P_\zeta(\omega) = \left\langle \left| \tilde{\zeta}(\omega) \right|^2 \right\rangle = \frac{8}{3\pi} \left(\frac{\tilde{G} M_X}{c v_{\rm DM}^2} \right)^2 \sin^2 \left(\frac{\omega L}{2c} \right) \times \left\{ \left[K_0 \left(\frac{D\omega}{v_{\rm DM}} \right) - K_0 \left(\frac{D'\omega}{v_{\rm DM}} \right) \right]^2 + \left[K_1 \left(\frac{D\omega}{v_{\rm DM}} \right) - K_1 \left(\frac{D'\omega}{v_{\rm DM}} \right) \right]^2 \right\} .$$